Journal of Inorganic Biochemistry 198 (2019) 110736

Contents lists available at ScienceDirect

Journal of Inorganic Biochemistry

journal homepage: www.elsevier.com/locate/jinorgbio

A suite of asymmetric citrate siderophores isolated from a marine *Shewanella* species

Jeffrey R. Carmichael, Hongjun Zhou, Alison Butler*

Department of Chemistry and Biochemistry, University of California, Santa Barbara, CA 93106-9510, United States of America

ARTICLE INFO

Keywords:
Shewanella woodyi MS32
Siderophore
Iron
Biosynthesis
NIS synthetase

ABSTRACT

Woodybactins A-D are a suite of new fatty acyl siderophores produced by the luminous marine bacterium *Shewanella woodyi* MS32. While this bacterium has a set of genes homologous to the biosynthetic gene cluster for aerobactin, aerobactin is not produced. The arrangement of these genes within the genome differs in *S. woodyi* MS32 when compared to *E. coli* and other species producing siderophores similar to aerobactin, and one synthetase gene which would append a second acyl-hydroxylysine to the terminal carboxylate of citrate is not functional. Within the suite of woodybactins A-D, which differ by the fatty acid appendage, one contains an unusual C_9 (9:0) fatty acid and one contains a unique branched C_9 iso (9:0 iso) fatty acid, as well as a C_8 (8:0) and C_{10} (10:0) fatty acid.

1. Introduction

Bacteria generally require iron to grow. Many bacteria produce siderophores, low molecular weight Fe(III) chelators, to facilitate iron uptake. Siderophores are synthesized by well-defined pathways encoded in the bacterial genome. Peptidic siderophores are synthesized by **n**on**r**ibosomal **p**eptide **s**ynthetase (NRPS) enzymes [1–3]. Non-peptidic siderophores, such as aerobactin (Fig. 1A), are synthesized by **N**RPS-**i**ndependent **s**iderophore (NIS) synthetases [4]. Aerobactin is produced by *E. coli* [5–6] as well as other pathogenic bacteria [7], plant pathogens [6], and marine *Vibrio* species [8–9]. In *E. coli*, aerobactin biosynthesis is encoded by the *iucABCD* gene cluster. IucD catalyzes the hydroxylation of the N^6 of L-lysine. IucB then catalyzes the N^6-acetylation of N^6-hydroxy-L-lysine. The synthetases IucA and IucC function sequentially to append N^6-acetyl-N^6-hydroxy-L-lysine to each terminal carboxylate of citrate, with IucA catalysis producing the S configuration at the central C-3 carbon of the citryl group (Fig. 1B) [4–5,10].

Ochrobactins A-C and ochrobactins-OH A-C are siderophores with structures resembling aerobactin, although both acetyl groups are replaced by fatty acids (Fig. 2) [11–12]. Fatty acid appendages, which are not uncommon in NIS siderophores, are also present in rhizobactin 1021 [13] and the synechobactins [14–15]. Most of the acylated citrate-derived siderophores are asymmetric about the C-3 center of the citryl group as a result of two different fatty acid appendages, although ochrobactin C and ochrobactin-OH B are symmetric. Homologs of aerobactin's *iucB* biosynthesis gene append a fatty acyl chain and acetyl group to hydroxy-diaminopropane during synthesis of rhizobactin 1021 [16], although the specificity of *iucB* homologs for the fatty acid vs an acetyl group has not been elucidated [13,16]. Branched fatty acids have yet to be reported in siderophores, and odd-chain fatty acids have only been reported for the synechobactins and the peptidic mycobactin siderophores [15,17].

NIS synthetases are divided into three subfamilies of enzymes: Type A, B, and C NIS synthetases. Type A synthetases are specific for citric acid, Type B for α-ketoglutaric acid, and Type C for derivatives of citrate or succinate [4,18]. Type A and C NIS synthetases are further divided into Types A, A′, C, and C′. Little distinction exists between the function of Types A and A′ NIS synthetases in that both typically catalyze amide bond formation between citric acid and an amine, although the Types A and A′ are phylogenetically distinct (see below). Types C and C′ also perform very similar functions through amide bond formation, although Type C′ enzymes are also known to oligomerize and cyclize citryl or succinyl derivatives, forming siderophores such as desferrioxamines, alcaligin, avaroferrin, and putrebactin [19–26].

Shewanella woodyi MS32 is a bioluminescent marine bacterium (Fig. S1) originally isolated from the Alboran Sea, and named in honor of J. Woodland ("Woody") Hastings, a legend in the field of photobiology [27]. The bioluminescence of *S. woodyi* MS32 is under quorum sensing control [27–29]. *S. woodyi* species produce relatively high amounts of iso fatty acids as compared to *Vibrio* or *Photobacterium* species, and odd-chain fatty acids have also been reported in *S. woodyi* species [27]. The unusual fatty acid production of *S. woodyi* could indicate the production

---

* Corresponding author.
E-mail address: butler@chem.ucsb.edu (A. Butler).

https://doi.org/10.1016/j.jinorgbio.2019.110736
Received 12 May 2019; Received in revised form 29 May 2019; Accepted 3 June 2019

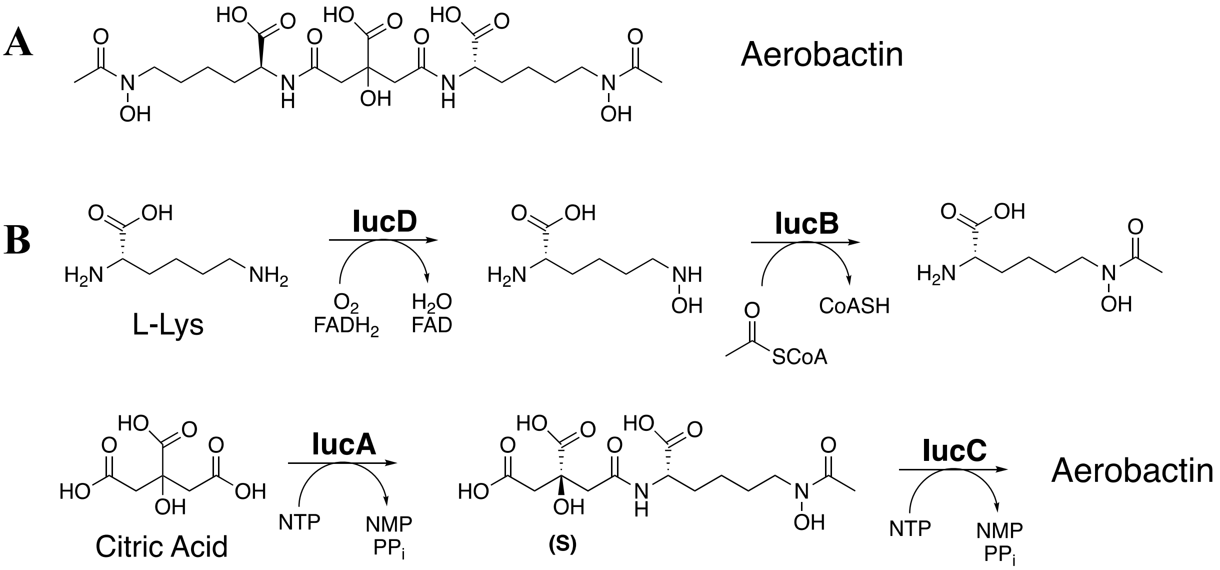

Fig. 1. A) Structure of aerobactin. B) Biosynthesis of aerobactin by IucABCD [4–5,10].

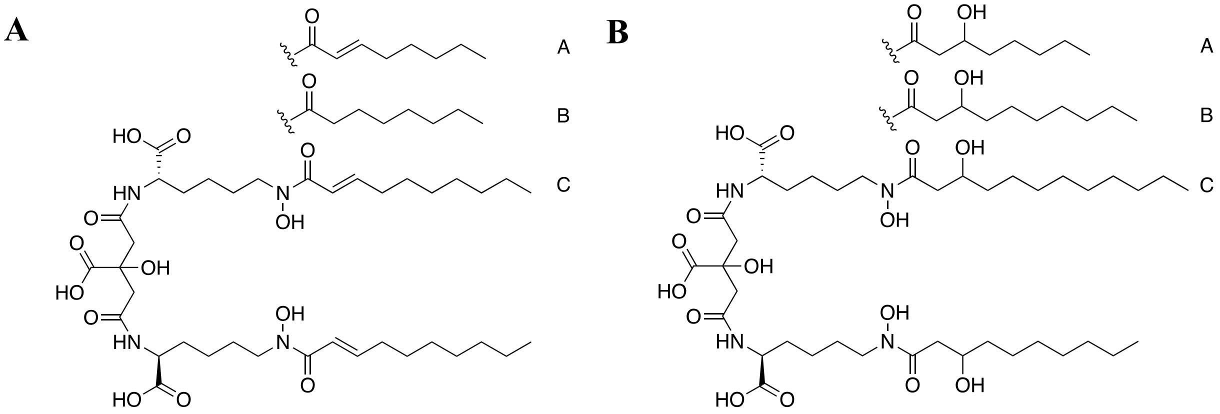

Fig. 2. Structure of A) ochrobactins A, B. and C [11], and B) ochrobactins-OH A, B, and C [12].

of novel fatty acid-containing metabolites.

The genome of *S. woodyi* MS32 contains genes homologous to the biosynthetic gene cluster for aerobactin, although the genes exist in a different spatial arrangement in the genome. Here we report the structures of woodybactins A-D, a suite of asymmetric citrate siderophores with structures similar to those of aerobactin, ochrobactins, and ochrobactins-OH, isolated from *Shewanella woodyi* MS32. Woodybactin C contains the uncommon C_9 (9:0) fatty acid, and woodybactin B contains a unique iso-branched C_9 (9:0 iso) fatty acid.

2. Materials and methods

2.1. General experimental procedures

All ^{1}H and two-dimensional (2D) NMR spectra were obtained at 25 °C using a Varian Inova 600 MHz NMR spectrometer equipped with an inverse detection probe. All ^{13}C NMR spectra were obtained at room-temperature (~23 °C) using a Varian Inova 500 MHz spectrometer equipped with a broadband probe. NMR samples were dissolved in dimethyl sulfoxide-d_6 (Cambridge Isotope Laboratories). All NMR spectra are referenced indirectly according to the signals from the solvent DMSO with the residual ^{1}H signal set to 2.54 ppm and ^{13}C signal set to 40.45 ppm. Molecular masses were determined using a Waters Xevo G2-XS QTof with positive mode electrospray ionization coupled to an ACQUITY UPLC-H-Class system with a Waters BEH C18 column. Samples were analyzed with a linear gradient of 0% to 100% CH_3CH (0.1% formic acid) in ddH_2O (0.1% formic acid) over 10 min.

2.2. Bacterial growth and isolation of siderophores

Shewanella woodyi MS32 was grown in 2 L of low-iron artificial seawater medium (ASG) containing 6 g Casamino acids, 30 g NaCl, 1.50 g KCl, 24 g $MgSO_4 \cdot 7H_2O$, 6 g $CaCl_2 \cdot 2H_2O$, 2 g NH_4Cl, 0.1 g Glycerol phosphate and 4 mL 1.0 M $NaHCO_3$ or Shewanella Marine Agar (SMA) containing (per liter) 5 g Bacto Peptone, 1 g Bacto Yeast Extract, 30.16 g NaCl, 5.08 g $MgCl_2 \cdot 6H_2O$, 6.16 g $MgSO_4 \cdot 7H_2O$, and 1.5 g KCl and brought to pH 7.5, with 15 g of bacto agar [27]. Media were inoculated with 5 mL of 2216 marine broth grown from a single colony of the bacterium isolated from a plate of SMA, shaken overnight at 180 rpm. The bacterial culture was grown on an orbital shaker at 180 rpm until it reached stationary phase as analyzed by the optical density at 600 nm versus growth time, at which point the cell culture gave a positive response to a chrome azurol-S (CAS) assay, indicating the potential presence of siderophores [30]. The culture was centrifuged (6000 rpm, 30 min, 4 °C) in an SLA-3000 rotor, the supernatant was decanted and mixed with ~200 mL (1/10 volume) of Amberlite XAD-2 resin (Supelco) and was shaken for ~4 h at 120 rpm, until supernatant tested CAS-negative. The XAD-2 resin was then filtered and rinsed with 2 L doubly-deionized H_2O (Barnstead Nanopure II), and the siderophores were eluted with 100% MeOH. The CAS-positive MeOH fractions were

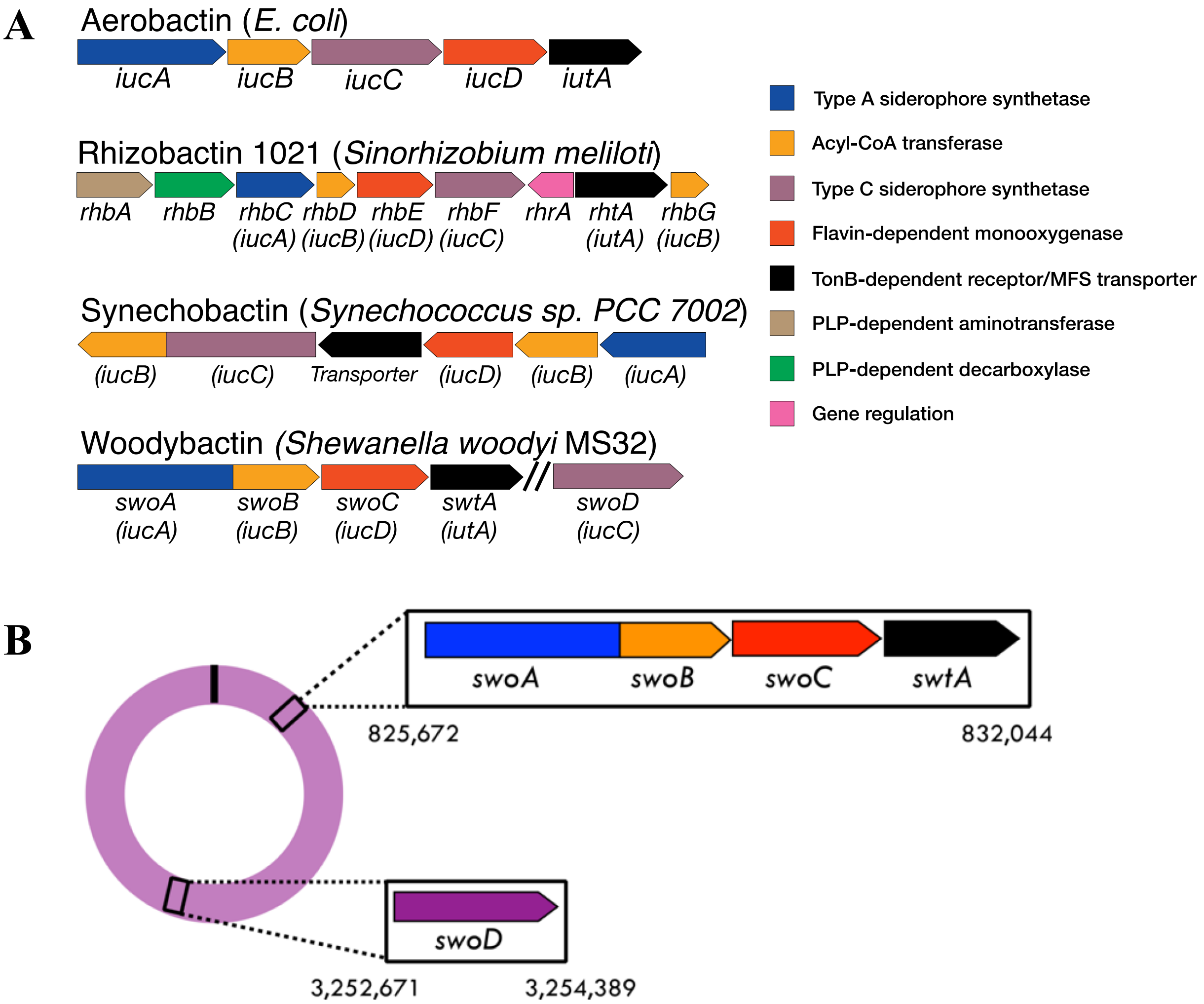

Fig. 3. A) Biosynthetic gene clusters of aerobactin and rhizobactin 1021, and predicted gene clusters of synechobactins (located on pAQ7 plasmid of *Synechococcus* sp. PCC7002) and woodybactins. The homologous genes to aerobactin in gene clusters of rhizobactin 1021 and woodybactin are placed in parentheses below the relevant gene. B) Relative locations of *swoABC*, *swtA*, and *swoD* in the *S. woodyi* MS32 genome.

consolidated and concentrated under vacuum to ~15 mL and were run through reverse-phase HPLC for purification using a gradient of 5% to 100% methanol over 50 min on a YMC 20 × 250 mm C18-AQ column. The cell pellets from centrifugation were resuspended in 70% ethanol (300 mL) and shaken at 4 °C for 24 h, at which point they were centrifuged (6000 rpm, 30 min, 4 °C) in an SLA-3000 rotor. The resulting supernatant was filtered through a 0.22 µm filter and concentrated under vacuum. The sample was then diluted in ~500 mL deionized H_2O and worked up with XAD-2 resin as described above.

3. Results and discussion

3.1. Genome mining

The genome of *S. woodyi* MS32 was screened for siderophore biosynthesis genes. While the genome lacks NRPS genes, it contains a set of genes homologous to *iucA*, *iucB*, *iucC*, and *iucD*, the cluster encoding biosynthesis of aerobactin, as well as *iutA*, the gene encoding the aerobactin transporter. However, the arrangement of the homologous genes in *S. woodyi* MS32, *swoA*, *swoB*, *swoC*, *swtA*, and *swoD*, differs from that in *E. coli* (Fig. 3A, Table S1). In particular the *iucC* homolog, *swoD*, resides nearly 2.5 million base pairs downstream from the gene cluster of *swoABC* and *swtA* (Fig. 3B).

Rhizobactin 1021 and the synechobactins are produced by NIS synthetases with homology to those of aerobactin [16,31] (Fig. 3A), although each citryl carboxylate group is derivatized with a different compound, producing asymmetric siderophores, unlike aerobactin. Rhizobactin 1021 and the synechobactins all have an acetyl appendage attached to hydroxy-diaminopropane on one side of the citryl group. On the opposing citryl carboxylate, rhizobactin 1021 has 2-decenoic acid appended to the hydroxy-diaminopropane [13], and the synechobactins have fatty acids ranging from 8:0 to 16:0 appended to the hydroxy-diaminopropane [14–15]. The biosynthetic gene clusters for rhizobactin 1021 and synechobactins each contain two *iucB* homologs, presumably one for the acetyl group and one for the fatty acids [4,16,31]. The genome of *S. woodyi* MS32 contains only one *iucB* homolog, *swoB*.

3.2. Structure determination

To isolate siderophores produced by *S. woodyi* MS32, the bacteria were grown as described in Materials and methods. The HPLC trace of the *S. woodyi* MS32 supernatant extract contains four peaks (Fig. 4), named here woodybactins A-D, which were identified as potential siderophores using the chrome azurol-S (CAS) assay [30]. Electrospray UPLC-MS analysis showed compounds A-D having molecular ion peaks of *m/z* 463, 477, 477, and 491, respectively, while the mass for aerobactin, *m/z* 565, was not observed [10]. The mass difference of 14 between 463, 477, and 491 suggests a potential difference of a single

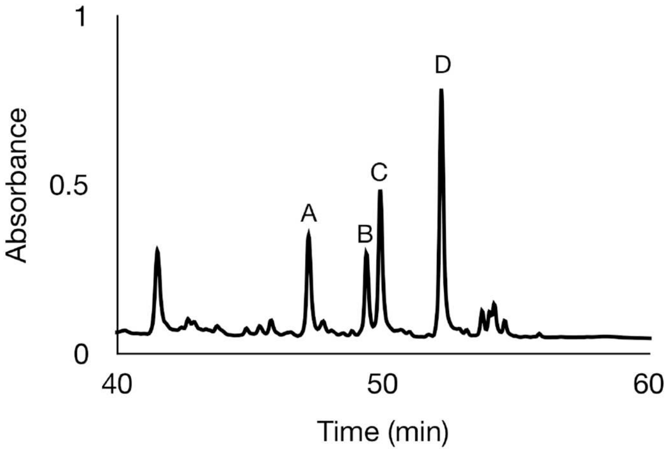

Fig. 4. HPLC chromatogram from supernatant of *S. woodyi* MS32. Sample is monitored at 215 nm.

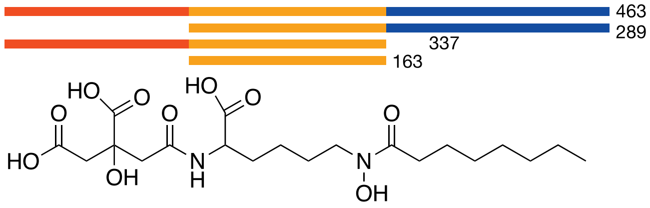

Fig. 5. Mass fragments of woodybactin A indicating a citrate appended by one acyl-hydroxylysine.

CH_2 group. All four compounds have similar fragmentation patterns below *m/z* 337 (Fig. S2), suggesting a major shared fragment between all of the woodybactins. The mass spectra of the woodybactins all share some fragments with the ochrobactins and ochrobactins-OH, including *m/z* 128, 145, and 163, which correspond to N^6-hydroxy-L-lysine [11–12]. Another indicative fragment for the woodybactins is N^6-hydroxy-L-lysine attached to an acyl group, indicated by the *m/z* 289 fragment in woodybactin A (also observed for ochrobactin B), m/z 303 in woodybactins B and C, and m/z 317 in woodybactin D (Figs. 5, S2–3) [11–12]. For aerobactin-producing species, the related N^6-acetyl-N^6-hydroxy-L-lysine fragment is observed (m/z 205) [9], which was not observed in extracts of *S. woodyi* MS32. These data suggest woodybactins A-D contain fatty acid chains of mostly varying length, with two having the same mass (Figs. 5, S2–3).

NMR of woodybactins A-D established the presence of citrate and hydroxylysine, each with a different fatty acid appendage (Fig. 6). All four siderophores have nearly identical resonances from C1 through C16 in both ^{13}C and ^{1}H NMR spectra (Tables 1, S2–S4). A triplet at 0.89 ppm integrates to 3 protons in the ^{1}H NMR spectra of woodybactins A, C, and D and couples to only CH_2 carbons in the HMBC (Heteronuclear Multiple Bond Correlation) spectrum, indicating these siderophores all consist of straight-chain fatty acids. Woodybactin A has a C_8 8:0 fatty acid, woodybactin C has a C_9 9:0 fatty acid, and woodybactin D has a C_{10} 10:0 fatty acid. The ^{1}H NMR spectrum of woodybactin B has a doublet at 0.88 ppm integrating to 6 protons (Table 1), corresponding to two CH_3 groups branched off of a CH, which was further confirmed through HMBC and COSY (Correlation Spectroscopy) (Figs. S11–12). Furthermore, although the two branched CH_3 resonances overlap, each CH_3 group of protons couples with the other methyl ^{13}C via three-bond *J* coupling, giving an intense resonance in the HMBC spectrum at the CH_3 resonance position. This coupling pattern is indicative of an iso-fatty acid, and represents the first instance of a siderophore containing a branched fatty acid. Odd-chain fatty acids, as in woodybactin B have only been reported in a few other siderophores [15,17].

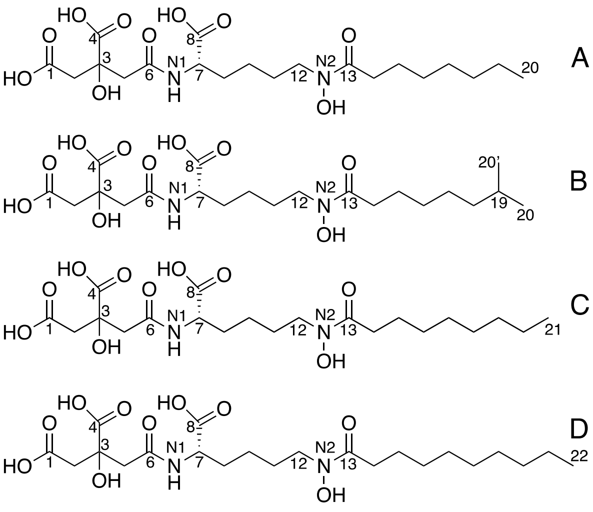

Fig. 6. Structures of woodybactins A-D.

3.3. Phylogenetic analysis of swoA and swoD

The phylogeny of the synthetase genes *swoA* and *swoD* was compared to other NIS synthetases with known functions (Fig. 7). The phylogenetic tree shows that *swoA* groups within the Type A clade alongside *iucA*, and *swoD* groups within the C′ clade with *iucC* (Fig. 7). Given the function of Type A NIS synthetases to condense an amine or alcohol with citric acid, SwoA is predicted to catalyze the formation of a monosubstituted citryl product. As a member of the Type C′ clade, SwoD is predicted to catalyze the condensation of an amine substituent to a monosubstituted citryl or succinyl group to form a disubstituted product [19].

The activity of SwoD in *S. woodyi* MS32 is not apparent given the lack of a disubstituted citryl product similar to aerobactin, ochrobactins, and ochrobactins-OH [11–12]. No siderophores containing a disubstituted citryl were found in either the cell pellet (extraction outlined in Materials and methods) or supernatant, which suggests that *swoD* is not operative in the biosynthesis of the woodybactins. However, unlike the other Type A NIS synthetases, SwoA appears to be attaching substrates with a range of fatty acid lengths to citric acid, indicating a relatively loose substrate specificity with respect to the nature of the fatty acids. The synechobactins contain a range of fatty acid lengths as well, which indicates a wide substrate specificity of its *iucA* homolog and potentially its two *iucB* homologs, although the biosynthesis of the synechobactins has not been extensively investigated [31]. The ochrobactins and ochrobactins-OH also contain a variety of fatty acid lengths, although the genomes of the bacteria which make them have not been published [11–12]. With more bacterial genomes being sequenced and made available, further investigations into these NIS biosynthetic pathways can hopefully soon be performed.

3.4. Fe(III) binding

Most siderophores coordinate Fe(III) with three bidentate ligands, commonly catechols, α-hydroxycarboxylic acids, and hydroxamic acids, with 1:1 stoichiometry. Some siderophores with two bidentate ligands, such as the bis hydroxamate putrebactin, and alcigin, bind Fe(III) with 1:1 or 2:3 Fe(III)-siderophore stoichiometry depending on pH conditions [25,39–41]. Unfortunately Fe(III) titration of woodybactin B was hampered by precipitation. However, under conditions of ~0.3 Fe(III):woodybactin B the UV–visible spectrum of Fe(III)-woodybactin B in 0.1 M phosphate buffer pH 7, shows an absorption maximum at ~420 nm with a shoulder at ~280 nm (Fig. S21), indicating coordination by both the hydroxamate and α-hydroxycarboxylate. Similar absorption maxima are observed for aerobactin [9]. UV photolysis of Fe

Table 1
NMR data of woodybactin B.

	δ_C, type	δ_H (J in Hz)	COSY	HMBC
1	172.2, C			
2	44.0, CH_2	2.68 m		1, 3, 4, 5
3	73.6, C			
4	175.7, C			
5	44.0, CH_2	2.68 m		2, 3, 4, 6
6	170.2, C			
N1		8.14 (d, 1H, J = 7.8)	7	6, 7
7	52.5, CH	4.17 (td, 1H, J = 5.1, 8.3)	N1, 9	8, 9
8	174.3, C			
9	31.7, CH_2	1.60 (m, 1H), 1.71 (m, 1H)	7, 10	7, 8, 10, 11
10	23.3, CH_2	1.30 m	9, 11	7, 9, 11, 12
11	26.9, CH_2	1.53 m	10, 12	9, 10, 12
12	47.8, CH_2	3.49 (t, 2H, J = 7.1 Hz)	11	10, 11, 13
N2				
13	173.6, C			
14	32.6, CH_2	2.36 (t, 2H, J = 7.6 Hz)	15	13, 15, 16
15	25.2, CH_2	1.51 m	14, 16	13, 14, 16, 17
16	30.0, CH_2	1.28 m	15	17, 18
17	27.6, CH_2	1.28 m	18	16, 18, 19
18	39.3, CH_2	1.17 (q, 2H, J = 6.9 Hz)	17, 20/20′	16, 17, 19, 20, 20′
19	28.3, CH	1.54 m		17, 18, 20, 20′
20, 20′	23.5, $2CH_3$	0.88 (d, 6H, J = 6.6 Hz)		18, 19, 20, 20′

(III)-woodybactin B leads to loss of 46 mass units, consistent with the coordination of α-hydroxy carboxylate to Fe(III) (Fig. S22) [9].

4. Conclusions

A suite of four fatty acyl siderophores, woodybactins A-D, have been isolated from *Shewanella woodyi* MS32. The woodybactins differ only in their fatty acid appendages, one of which, woodybactin C, has an uncommon odd-chain 9:0 fatty acid, one of which, woodybactin B, has a 9:0 iso branched fatty acid. Iso branched fatty acids have not been reported previously in siderophores.

The woodybactin structures were partially predicted through genome mining of *S. woodyi* MS32. The genome contains the biosynthesis genes *swoABC* and *swoD*, and the siderophore transporter *swtA*. The *swoABC* and *swoD* genes are homologous to the biosynthesis genes for aerobactin, *iucABCD*. SwoA is a Type A siderophore synthetase closely related to IucA, whose function is to append N^6-acetyl-N^6-hydroxy-L-lysine to a citryl group, which gives us woodybactins A-D. SwoD is a Type C′ siderophore synthetase closely related to IucC, and is predicted to append a second N^6-acetyl-N^6-hydroxy-L-lysine, the monosubstituted citryl product of SwoA. The absence of a disubstituted citryl siderophore from *S. woodyi* MS32 indicates *swoD* is not functional with *swoABC*.

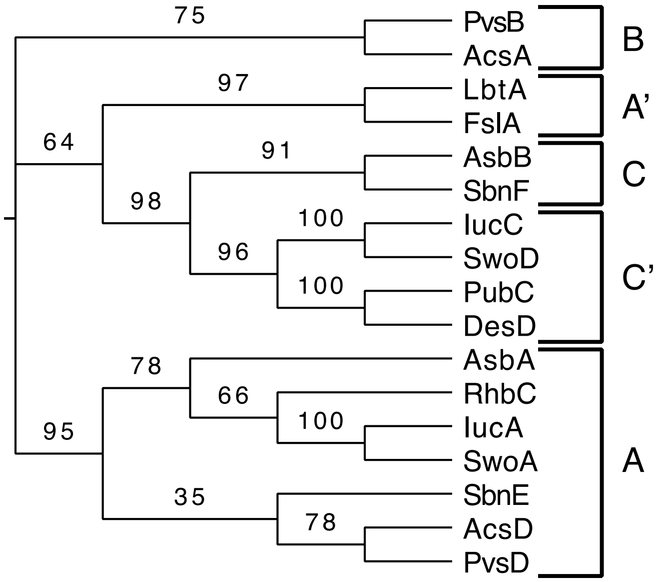

Fig. 7. Phylogenetic analysis of several common NIS synthetases. AcsA and AcsD - achromobactin biosynthesis [32]; AsbA and AsbB - petrobactin biosynthesis [33]; DesD - desferrioxamine biosynthesis [34]; FslA - rhizoferrin biosynthesis [35]; IucA and IucC - aerobactin biosynthesis [5]; SwoA and SwoD - woodybactin biosynthesis (this work); LbtA - legiobactin biosynthesis [36]; PubC - putrebactin biosynthesis [24]; PvsB and PvsD - vibrioferrin biosynthesis [37]; RhbC - rhizobactin 1021 biosynthesis [16]; SbnE and SbnF - staphyloferrin B biosynthesis [38].

Acknowledgments

We thank Prof. Jeffrey Gralnick (University of Minnesota) for the sample of *Shewanella woodyi* MS32. A.B. gratefully acknowledges support from NSF CHE-1710761.

Appendix A. Supplementary data

Supplementary data to this article can be found online at https://doi.org/10.1016/j.jinorgbio.2019.110736.

References

[1] M.A. Marahiel, T. Stachelhaus, H.D. Mootz, Modular peptide synthetases involved in nonribosomal peptide synthesis, Chem. Rev. 97 (7) (1997) 2651–2674.

[2] T. Stachelhaus, H.D. Mootz, M.A. Marahiel, The specificity-conferring code of adenylation domains in nonribosomal peptide synthetases, Chem. Biol. 6 (8) (1999) 493–505.

[3] J. Grünewald, M.A. Marahiel, Chemoenzymatic and template-directed synthesis of bioactive macrocyclic peptides, Microbiol. Mol. Biol. Rev. 70 (1) (2006) 121–146.

[4] G.L. Challis, A widely distributed bacterial pathway for siderophore biosynthesis independent of nonribosomal peptide synthetases, ChemBioChem 6 (4) (2005) 601–611.

[5] V. de Lorenzo, A. Bindereif, B.H. Paw, J.B. Neilands, Aerobactin biosynthesis and transport genes of plasmid ColV-K30 in Escherichia coli K-12, J. Bacteriol. 165 (2) (1986) 570–578.

[6] J.B. Neilands, Mechanism and regulation of synthesis of aerobactin in Escherichia coli K12 (pColV-K30), Can. J. Microbiol. 38 (7) (1992) 728–733.

[7] F. Gibson, D.I. Magrath, The isolation and characterization of a hydroxamic acid (aerobactin) formed by Aerobacter aerogenes 62-I, Biochim. Biophys. Acta 192 (2) (1969) 175–184.

[8] M.G. Haygood, P.D. Holt, A. Butler, Aerobactin production by a planktonic marine Vibrio sp. Limnol. Oceanogr. 38 (5) (1993) 1091–1097.

[9] F.C. Küpper, C.J. Carrano, J.-U. Kuhn, A. Butler, Photoreactivity of iron (III) – aerobactin: photoproduct structure and iron(III) coordination, Inorg. Chem. 45 (15) (2006) 6028–6033.

[10] D.C. Bailey, E. Alexander, M.R. Rice, E.J. Drake, L.S. Mydy, C.C. Aldrich, A.M. Gulick, Structural and functional delineation of aerobactin biosynthesis in hypervirulent Klebsiella pneumoniae, J. Biol. Chem. 293 (20) (2018) 7841–7852.

[11] J.D. Martin, Y. Ito, V.V. Homann, M.G. Haygood, A. Butler, Structure and membrane affinity of new amphiphilic siderophores produced by Ochrobactrum sp. SP18, JBIC, J. Biol. Inorg. Chem. 11 (5) (2006) 633–641.

[12] J.M. Gauglitz, H. Zhou, A. Butler, A suite of citrate-derived siderophores from a marine Vibrio species isolated following the Deepwater Horizon oil spill, J. Inorg. Biochem. 107 (1) (2012) 90–95.

[13] M. Persmark, P. Pittman, J.S. Buyer, B. Schwyn, P.R. Gill, J.B. Neilands, Isolation and structure of rhizobactin 1021, a siderophore from the alfalfa symbiont Rhizobium meliloti 1021, J. Am. Chem. Soc. 115 (10) (1993) 3950–3956.

[14] Y. Ito, A. Butler, Structure of synechobactins, new siderophores of the marine cyanobacterium Synechococcus sp. PCC 7002, Limnol. Oceanogr. 50 (6) (2005) 1918–1923.

[15] R.M. Boiteau, D.J. Repeta, An extended siderophore suite from Synechococcus sp. PCC 7002 revealed by LC-ICPMS-ESIMS, Metallomics 7 (5) (2015) 877–884.

[16] D. Lynch, J. O'Brien, T. Welch, P. Clarke, P.O. Cuív, J.H. Crosa, M. O'Connell, Genetic organization of the region encoding regulation, biosynthesis, and transport of rhizobactin 1021, a siderophore produced by Sinorhizobium meliloti, J. Bacteriol. 183 (8) (2001) 2576–2585.

[17] G.A. Snow, Mycobactins: iron-chelating growth factors from mycobacteria, Bacteriol. Rev. 34 (2) (1970) 99–125.

[18] D. Oves-Costales, N. Kadi, G.L. Challis, The long-overlooked enzymology of a nonribosomal peptide synthetase-independent pathway for virulence-conferring siderophore biosynthesis, Chem. Commun. (43) (2009) 6530–6541.

[19] M.M. Moore, Ironing out siderophore biosynthesis: a review of non-ribosomal peptide synthetase (NRPS)-independent siderophore synthetases AU – Carroll Cassandra S, Crit. Rev. Biochem. Mol. Biol. 53 (4) (2018) 356–381.

[20] Karimi, K. L.; Hoffmann, K. M., Determining the Structure of NRPS-Independent Siderophore (NIS) Synthetase DesD Using X-ray Crystallography. FASEB J. 2016, *30* (1_supplement), 836.4–836.4.

[21] S. Rütschlin, T. Böttcher, Dissecting the mechanism of oligomerization and macrocyclization reactions of NRPS-independent siderophore synthetases, Chem. Eur. J. 24 (60) (2018) 16044–16051.

[22] T. Nishio, N. Tanaka, J. Hiratake, Y. Katsube, Y. Ishida, J. Oda, Isolation and structure of the novel dihydroxamate siderophore alcaligin, J. Am. Chem. Soc. 110 (26) (1988) 8733–8734.

[23] P.C. Giardina, L.-A. Foster, S.I. Toth, B.A. Roe, D.W. Dyer, Analysis of the alcABC operon encoding alcaligin biosynthesis enzymes in Bordetella bronchiseptica, Gene 194 (1) (1997) 19–24.

[24] N. Kadi, S. Arbache, L. Song, D. Oves-Costales, G.L. Challis, Identification of a gene cluster that directs putrebactin biosynthesis in Shewanella species: PubC catalyzes cyclodimerization of N-hydroxy-N-succinylputrescine, J. Am. Chem. Soc. 130 (32) (2008) 10458–10459.

[25] R. Codd, C.Z. Soe, A.A.H. Pakchung, A. Sresutharsan, C.J.M. Brown, W. Tieu, The chemical biology and coordination chemistry of putrebactin, avaroferrin, bisucaberin, and alcaligin, JBIC, J. Biol. Inorg. Chem. 23 (7) (2018) 969–982.

[26] R. Codd, T. Richardson-Sanchez, T.J. Telfer, M.P. Gotsbacher, Advances in the chemical biology of desferrioxamine B, ACS Chem. Biol. 13 (1) (2018) 11–25.

[27] J.C. Makemson, N.R. Fulayfil, W. Landry, L.M. Van Ert, C.F. Wimpee, E.A. Widder, J.F. Case, Shewanella woodyi sp. nov., an exclusively respiratory luminous bacterium isolated from the Alboran Sea, Int. J. Syst. Evol. Microbiol. 47 (4) (1997) 1034–1039.

[28] N. Liu, Y. Xu, S. Hossain, N. Huang, D. Coursolle, J.A. Gralnick, E.M. Boon, Nitric oxide regulation of cyclic di-GMP synthesis and hydrolysis in Shewanella woodyi, Biochemistry 51 (10) (2012) 2087–2099.

[29] X. Tian, F. Zhao, L. You, X. Wu, Z. Zheng, R. Wu, Y. Jiang, S. Sun, Interaction between in vivo bioluminescence and extracellular electron transfer in Shewanella woodyi via charge and discharge, Phys. Chem. Chem. Phys. 19 (3) (2017) 1746–1750.

[30] B. Schwyn, J.B. Neilands, Universal chemical assay for the detection and determination of siderophores, Anal. Biochem. 160 (1) (1987) 47–56.

[31] M. Ludwig, D.A. Bryant, Acclimation of the global transcriptome of the cyanobacterium Synechococcus sp. strain PCC 7002 to nutrient limitations and different nitrogen sources, Front. Microbiol. 3 (2012) 1–15.

[32] A.D. Berti, M.G. Thomas, Analysis of achromobactin biosynthesis by Pseudomonas syringae pv. syringae B728a, J. Bacteriol. 191 (14) (2009) 4594–4604.

[33] J.Y. Lee, B.K. Janes, K.D. Passalacqua, B.F. Pfleger, N.H. Bergman, H. Liu, K. Håkansson, R.V. Somu, C.C. Aldrich, S. Cendrowski, P.C. Hanna, D.H. Sherman, Biosynthetic analysis of the petrobactin siderophore pathway from Bacillus anthracis, J. Bacteriol. 189 (5) (2007) 1698.

[34] F. Barona-Gómez, U. Wong, A.E. Giannakopulos, P.J. Derrick, G.L. Challis, Identification of a cluster of genes that directs desferrioxamine biosynthesis in Streptomyces coelicolor M145, J. Am. Chem. Soc. 126 (50) (2004) 16282–16283.

[35] J.T. Sullivan, E.F. Jeffery, J.D. Shannon, G. Ramakrishnan, Characterization of the siderophore of Francisella tularensis and role of fslA in siderophore production, J. Bacteriol. 188 (11) (2006) 3785–3795.

[36] K.A. Allard, V.K. Viswanathan, N.P. Cianciotto, lbtA and lbtB are required for production of the Legionella pneumophila siderophore legiobactin, J. Bacteriol. 188 (4) (2006) 1351–1363.

[37] T. Tanabe, T. Funahashi, H. Nakao, S.-I. Miyoshi, S. Shinoda, S. Yamamoto, Identification and characterization of genes required for biosynthesis and transport of the siderophore vibrioferrin in Vibrio parahaemolyticus, J. Bacteriol. 185 (23) (2003) 6938–6949.

[38] J. Cheung, F.C. Beasley, S. Liu, G.A. Lajoie, D.E. Heinrichs, Molecular characterization of staphyloferrin B biosynthesis in Staphylococcus aureus, Mol. Microbiol. 74 (3) (2009) 594–608.

[39] K.M. Ledyard, A. Butler, Structure of putrebactin, a new dihydroxamate siderophore produced by Shewanella putrefaciens, JBIC, J. Biol. Inorg. Chem. 2 (1) (1997) 93–97.

[40] Z. Hou, C.J. Sunderland, T. Nishio, K.N. Raymond, Preorganization of ferric alcaligin, Fe2L3. The first structure of a ferric dihydroxamate siderophore, J. Am. Chem. Soc. 118 (21) (1996) 5148–5149.

[41] Z. Hou, K.N. Raymond, B. O'Sulliva, T.W. Esker, T. Nishio, A preorganized siderophore: thermodynamic and structural characterization of alcaligin and bisucaberin, microbial macrocyclic dihydroxamate chelating agents, Inorg. Chem. 37 (26) (1998) 6630–6637.